JCTC Journal of Chemical Theory and Computation

Article

pubs.acs.org/JCTC

Transition-Tempered Metadynamics: Robust, Convergent Metadynamics via On-the-Fly Transition Barrier Estimation

James F. Dama,[†] Grant Rotskoff,[†,∥] Michele Parrinello,[‡,§] and Gregory A. Voth*[,†]

[†]Department of Chemistry, James Franck Institute, Institute for Biophysical Dynamics, and Computation Institute, The University of Chicago, Chicago, Illinois 60637, United States

[‡]Department of Chemistry and Applied Biosciences, ETH Zurich, Zürich, Switzerland

[§]Facoltà di Informatica, Istituto di Scienze Computazionali, Università della Svizzera Italiana, Via G. Buffi 13, 6900 Lugano, Switzerland

Supporting Information

ABSTRACT: Well-tempered metadynamics has proven to be a practical and efficient adaptive enhanced sampling method for the computational study of biomolecular and materials systems. However, choosing its tunable parameter can be challenging and requires balancing a trade-off between fast escape from local metastable states and fast convergence of an overall free energy estimate. In this article, we present a new smoothly convergent variant of metadynamics, transition-tempered metadynamics, that removes that trade-off and is more robust to changes in its own single tunable parameter, resulting in substantial speed and accuracy improvements. The new method is specifically designed to study state-to-state transitions in which the states of greatest interest are known ahead of time, but transition mechanisms are not. The design is guided by a picture of adaptive enhanced sampling as a means to increase dynamical connectivity of a model's state space until percolation between all points of interest is reached, and it uses the degree of dynamical percolation to automatically tune the convergence rate. We apply the new method to Brownian dynamics on 48 random 1D surfaces, blocked alanine dipeptide *in vacuo*, and aqueous myoglobin, finding that transition-tempered metadynamics substantially and reproducibly improves upon well-tempered metadynamics in terms of first barrier crossing rate, convergence rate, and robustness to the choice of tuning parameter. Moreover, the trade-off between first barrier crossing rate and convergence rate is eliminated: the new method drives escape from an initial metastable state as fast as metadynamics without tempering, regardless of tuning.

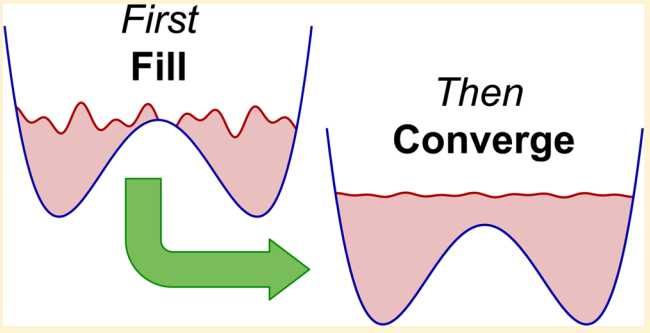

1. INTRODUCTION

Molecular dynamics has become a powerful tool for studying the dynamics and statics of many-particle chemical systems.[1−3] However, many observables of interest are averages over the equilibrium distribution of particle configurations, and pure molecular dynamics can be an inefficient tool for calculating such averages. It can be much more efficient to use enhanced sampling methods that adapt the core trajectory sampling functionality of molecular dynamics to the problem of sampling configurational averages.[4−6]

This paper introduces a new enhanced sampling method for calculating potentials of mean force along a few well-chosen collective variables (CVs) at a time, transition-tempered metadynamics (TTMetaD), which appears to offer significant advantages in accuracy, precision, and robustness over the most closely comparable state of the art methods. It is one of a long progression of enhanced sampling methods designed to calculate potentials of mean force (PMFs) of several CVs using the least foreknowledge of the system necessary. It is worth placing it in context with these other enhanced sampling methods before introducing it by tracing the history of its antecedents.

One of the earliest and best known enhanced sampling methods is umbrella sampling,[7,8] in which one or more bias potentials are added to an otherwise normal molecular dynamics simulation to encourage sampling of high-free-energy configurations that otherwise act as kinetic barriers. By ameliorating these barriers, umbrella sampling makes calculation of averages of quantities that require high quality sampling across the barrier more efficient. Two basic classes of umbrella sampling are typical. In the first, a single potential is added to flatten out the free energy surface around and across the barrier. To engineer such a potential requires knowing the approximate location and free energy surface of the barrier region. In another, simulations are run under many different so-called window potentials to ensure that sampling of each so-called window—including the ones around the barrier—is of roughly even quality. To engineer these requires knowing the

Received: May 21, 2014
Published: July 23, 2014

   dx.doi.org/10.1021/ct500441q | J. Chem. Theory Comput. 2014, 10, 3626−3633

approximate free energy gradients around the barrier. Unfortunately, the free energies, locations, and shapes of the barriers are often exactly what one wants to discover.

When very little information about the barrier is known in advance, an alternative is to bootstrap an umbrella potential by starting with unbiased molecular dynamics and iteratively biasing the dynamics as more becomes known.[9,10] Metadynamics[11−13] is an archetypal method of this type meant to take only a few reaction coordinates and information about their short-time dynamic fluctuations as inputs. Alternatives include Adaptive Biasing Force[14,15] and Wang−Landau[16] methods, and its most immediate precursor was the Local Elevation Method.[17] In metadynamics, as in the Local Elevation Method, the simulation begins unbiased and the system is sequentially biased away from the neighborhood of the points it has already visited in reaction coordinate space. This bias builds cumulatively until all reaction coordinate points are equally likely to be sampled—at least in concept. In reality, one must taper the incremental bias additions to zero to achieve true convergence, which was the inspiration for well-tempered metadynamics (WTMetaD).[18]

WTMetaD adds increments of bias that smoothly taper to zero as the bias grows across the reaction coordinate space to ensure that the bias does eventually converge to the desired umbrella potential. It has close connections with the Wang−Landau $1/t$ method[19] and the Robbins-Munro algorithm[20] in that the size of WTMetaD updates asymptotically decays as $1/t$.[21,22] Unfortunately, in WTMetaD the tapering rate is set using a tuning parameter that should match the barrier height to be overcome, reintroducing a requirement for information that metadynamics was initially designed to do without. Furthermore, bias updates, hereafter referred to as added hills, are tapered from the start to achieve long-time convergence, forcing researchers to make trade-offs between the time until they see the first barrier crossing events and the asymptotic convergence rate. Higher tapering can accelerate convergence but will slow escape from basins. Since barrier crossings are often an important preliminary sign of whether or not the method is working but a converged free energy is the final goal, this is not a pleasant trade-off to accept.

This paper presents a new metadynamics method, TTMetaD, that is smoothly convergent like WTMetaD and the $1/t$ method but does not require foreknowledge of the barrier height and avoids the trade-off between fast barrier crossings and fast convergence. Instead, it asks only for approximate basin positions and decreases the height of added hills roughly according to the number of round trips between the basins. The basins can be chosen using a combination of experimental data and physical insight, for instance crystal structures of different conformers, FRET measurements, or intuition for peptide bond angles, and they will typically be a subset of only a few of the total number of basins in the system, chosen based on the goals of the metadynamics investigation. It is an asymptotically convergent method like WTMetaD, and in the examples we have examined it consistently and substantially improves upon WTMetaD in terms of both barrier crossing rates and convergence rates.

2. METHOD

TTMetaD is inspired by an elegantly idealized picture of metadynamics developed by Laio et al.[23] and Bussi et al.[24] These works showed that metadynamics can profitably be thought of as a two-stage process. In the first stage, hills of bias fill the basins in the energy landscape to the point that the biased landscape has a uniform roughness set by the size of the hills added. After this point is reached, in the second stage the biased landscape fluctuates indefinitely, keeping that characteristic roughness indefinitely as well. In this picture, tempering the hills—decreasing the size of added hills as time goes on—is a way of ensuring that the characteristic roughness of the fluctuating bias eventually falls to zero so that the biased surface becomes perfectly flat. Tempering shortens the second phase because it decreases the characteristic roughness but lengthens the first phase because it decreases the basin filling rate. TTMetaD is designed to minimize the overall runtime of the method by ensuring that the hills are not tempered at all in the first phase, making that phase as short as possible, but also that they are still tempered properly in the second phase, making that phase also as short as possible.

Accomplishing this design requires some automatic way to recognize that the second phase has begun, and its definition provides a natural choice: the second phase occurs when all of the major basins of the PMF are filled by the bias and the biases filling them link up across the transition regions between them. Put differently, given a PMF with a few major basins, the second phase begins once there are paths between all of those basins that never cross a region in which the bias is zero. In fact, we can go further and measure the amount of overfilling quantitatively as the minimum bias on the maximally biased path between the basins; call this V^*. As long as the biases filling the basins are not connected, V^* remains zero, because any path between the basins must enter an unbiased region, and it grows steadily after the connections are established.

In the two-phase picture of metadynamics, the more overfilled the basins are, the smaller the hills should be. This provides a recipe for TTMetaD. The recipe follows our work on the convergence of metadynamics[22] and the example of WTMetaD, in which tempering is achieved by replacing the hill height h with $h\,e^{-V(s(t),t)/\Delta T}$ everywhere it appears. $V(s(t),t)$ is the bias at the CV-space point $s(t)$ sampled at time t; s may be a discrete number, a continuous number, a vector, a function, or a combination of all of these. ΔT is the tuning parameter discussed in the Introduction that sets the speed of convergence. In TTMetaD, we replace h with $h\,e^{-V^*(t)/\Delta T}$ everywhere it appears. This is a special case of globally tempered metadynamics as defined in our convergence work because in the notation of that paper $e^{-V^*(t)/\Delta T} = e^{-\bar{V}(t)/\Delta T}\,e^{-\tilde{V}^*(t)/\Delta T}$ and $e^{-\tilde{V}^*(t)/\Delta T}$ is a positive-valued functional of the driving bias $\tilde{V}$ alone. Using an exponential form like this ensures that the updates for TTMetaD decay as $1/t$ asymptotically like WTMetaD, Wang−Landau $1/t$ methods,[19] and Robbins-Munro.[20] That guarantees asymptotic convergence.[22]

That suffices to describe the essence of the method. The remainder of this section discusses technical details, providing explicit equations for the update rule and describing our software implementation.

First, we define V^*. We will give two definitions, one which is more intuitive and the second of which is less clear but is completely unambiguous once understood. V^* as introduced above is the minimum bias on the maximally biased path between all basins of interest. These basins of interest are specified in advance by defining a set of n CV coordinates s_b, where b is a basin index. For instance, in the case of an A to B transition, n will be 2, s_A and s_B, no matter how many

dx.doi.org/10.1021/ct500441q | J. Chem. Theory Comput. 2014, 10, 3626−3633

intervening basins are involved in the transition mechanism. These s_b's are points within each basin of interest and need not be the minimum-energy points in each basin. Given a bias surface $V(s)$, we can then look at paths $s(\lambda)$, with $\lambda \in [0,1]$ a path progress variable, that link all of the points s_b, then pick out one that is maximally biased, $s^*(\lambda)$. Then V^* is the minimum bias on the path $s^*(\lambda)$.

Examine once more how this definition detects the transition between the initial filling phase and the second convergence phase of tempered metadynamics. In the initial phase, the bias will not entirely fill all of the basins. Therefore, the bias surface looks like a number of hills, corresponding to partially filled basins, separated by regions where the bias is zero. Any path between the hills must pass through a region where the bias is zero, so V^* must also be zero. As the filling stage continues, these initially fully separated hills start to overlap, but V^* still remains zero until every one of the bias hills corresponding to basins chosen by s_b is nonzero and overlaps with basins that connect up with the others. This behavior guarantees that there is no need to know in advance where the barrier is, which basins will fill first, or anything more than the rough locations of the basins of interest in order to detect the end of the initial filling phase. It also gives a clear picture of how roughly those basin locations can be defined: so long as the basin-defining coordinate s_b is within a reasonable isosurface of free energy around the true basin minimum, say half the barrier-basin free energy difference, then it will work well for TTMetaD. This is very permissive.

Now we unambiguously define what is meant by maximally biased path. First define the uncountable set $\mathcal{P}$ of all continuous paths $s(\lambda)$ that pass through all of the selected basin points s_b in the landscape; $\lambda \in [0,1]$ indexes the points along the path from start ($\lambda = 0$) to finish ($\lambda = 1$) as before. Then

$$V^*(t) \equiv \max_{s(\lambda)\in\mathcal{P}} \min_{\lambda\in[0,1]} V(s(\lambda), t) \tag{1}$$

In other words, maximally biased paths are those for which the minimum bias is maximal. Since this definition allows for many possible equally maximally biased paths, there is some flexibility in choosing $s^*(\lambda)$, e.g., $s^*(\lambda)$ may or may not have any number of loops within the individual already-filled basins. However, even though multiple $s^*(\lambda)$'s might be possible, V^* is always defined unambiguously by this definition. It suffices to find any single $s^*(\lambda)$ to find V^*.

Because metadynamics is stochastic, it will sometimes be possible that bias connects across the transition regions before the basins are fully filled. To guard against that possibility, we can add a bias threshold that serves to delay tempering until multiple crossings have occurred. Thresholded TTMetaD (ThTTMetaD) replaces $V^*(t)$ with $\max(V^*(t) - V_{th}, 0)$ everywhere it appears, where V_{th} is an adjustable parameter. It works to increase the robustness of the method because decreasing the hill height too early is generally more costly than waiting slightly later to enter the convergence phase. However, as we show later it was inessential in our tests; we have included it here primarily for the sake of completeness. Note that ThTTMetaD could also be used as a method for exploring a single basin up to a roughly specified free energy level—one can choose two points in the same basin as the end points of the transition and then choose the threshold bias value to match the desired free energy level.

The optimal choices of ΔT and V_{th} are no longer directly tied to the magnitude of the energy barrier and are quite robust, as we will show below, but they may still be fine-tuned for each system. Because they control convergence rate, it is intuitive that they should be matched to the natural sampling time scales of the method after bias has filled the main basins. Each energy parameter can be converted to a time scale using the hill energy addition rate h/τ_{revisit}, where τ_{revisit} is the characteristic time between adding hills to the highest barrier point between the basins, to convert from energy to time. One should choose $\tau_{\text{revisit}}\Delta T/h$ and optionally $\tau_{\text{revisit}}V_{th}/h$ so that they are comparable to the longest important relaxation time scales in the almost-converged biased system. If they are chosen to be longer, then the method will not converge as quickly as it could. If they are chosen shorter, then the method will appear to converge too early but will in fact be biased by the initial conditions, and the bias may take a long time to converge to zero. These time scales will typically be related to physics not included in the CVs, the so-called orthogonal variable relaxations. Though this may seem harder to discover than the barrier energy for WTMetaD, in fact fine-tuning WTMetaD must also take this into account, so there is no disadvantage here—we have simply made the difficulty of fine-tuning more apparent because the coarse-tuning is performed automatically.

Next, like WTMetaD, TTMetaD can also be used with sophisticated hill types: see adaptive Gaussian metadynamics,[21] boundary-consistent metadynamics,[25] or field-coordinate metadynamics[26] for examples. Whatever the case, the metadynamics rule without tempering is to deposit a bias hill with the functional form $G(s, s(t_n))$ when point $s(t_n)$ is sampled at time t_n. With these defined, the final iterative TTMetaD rule with generic hills and thresholding is

$$V(s, t_{n+1}) = V(s, t_n) + e^{-\max(V^*(t_n)-V^{th},0)/\Delta T} G(s, s(t_{n+1})) \tag{2}$$

With Gaussian hills of width δ and height h, this is

$$V(s, t_{n+1}) = V(s, t_n) + h\, e^{-\max(V^*(t_n)-V^{th},0)/\Delta T} e^{-\|s-s(t_{n+1})\|^2/2\delta^2} \tag{3}$$

Properly tempered metadynamics methods converge to biases V_c for which the expected bias update is flat. In TTMetaD, those biases satisfy

$$\int_S e^{-\max(V^*-V^{th},0)/\Delta T} G(s, s(t_n))\, e^{-(F(s(t_n))+V_c(s(t_n)))/T}\, ds(t_n) = C \tag{4}$$

$$\int_S G(s, s(t_n))\, e^{-(F(s(t_n))+V_c(s(t_n)))/T}\, ds(t_n) = C' \tag{5}$$

where $F(s)$ is the true CV PMF. For standard hills, such as Gaussians on a periodic domain or boundary-corrected Gaussians on a finite domain, requiring $\int_S G(s, s_n) \exp(-(F(s_n) + V_c(s_n)/T)\, ds_n$ to be flat requires that $\exp(-(F(s_n) + V_c(s_n)/T)$ must also be flat. Therefore, in these normal cases the final converged bias for the method is $V_c(s) = -F(s)$. This is exactly the target of the original metadynamics, making the bias easy to interpret and fully compatible with existing metadynamics postprocessing tools and workflows.

We implemented this method in PLUMED,[27] a cross-platform enhanced sampling plug-in for running enhanced sampling calculations in a number of molecular dynamics packages including Gromacs,[28] LAMMPS,[29] and NAMD,[30]

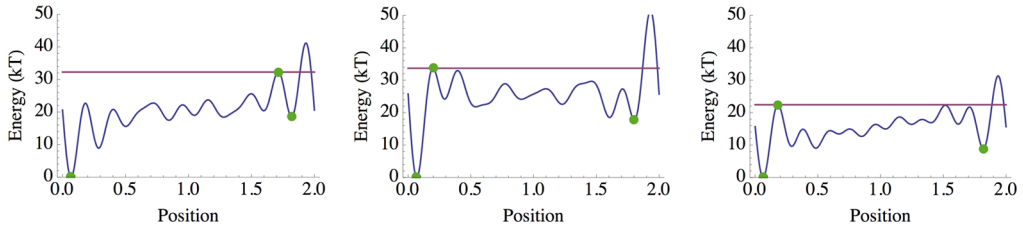

Figure 1. Three characteristic examples of potentials in the test set of 48 used to compare TTMetaD and WTMetaD in this section. Blue lines denote the potential surface, while green dots indicate the leftmost basin from which dynamics was initialized, the rightmost basin used as the second target basin, and the highest barrier between the two, and the red lines mark the barrier energy level. The test set includes potentials with early barriers, late barriers, and both early and late barriers.

among others. Our code is freely available on request. The implementation required minimal changes mostly consisting of added algorithms for calculation of the V^* and added code to set hill height based on $e^{-V^*(t)/\Delta T}$ rather than $e^{-V(s(t))/\Delta T}$. We calculate V^* to a close approximation by using Dijkstra's algorithm[31] to find paths of minimum cost $s^*(\lambda)$ between every pair of basins on a finely sampled grid of the bias. The basins are specified as specific points picked to be within the basins based on foreknowledge of the system, e.g., an *apo* crystal structure and a *holo* crystal structure for a ligand-binding protein. The path cost function used in the Dijkstra's algorithm computation is the negative of the minimum bias along the path, and thus negative of the maximum final path cost can be used as an estimate of $V^*(t)$. More sophisticated path finding algorithms would offer superior performance, but in our test cases we found that even this path finding calculation is so fast compared to force-field evaluation that the performance cost is negligible in practice. Specific numbers are provided with the test results below where applicable.

3. RESULTS AND DISCUSSION

The TTMetaD method is designed to improve upon well-tempered metadynamics in three areas. It is meant to be more robust to changes in parameters, to offer superior asymptotic convergence rates, and to explore phase space more efficiently at early times. We performed three sets of tests to verify that these goals were met. First, we studied the behavior of TTMetaD and WTMetaD on an ensemble of 1D systems to compare robustness, convergence, and fast barrier crossing in an idealized setting where many replicates can be performed with analytic target results. Second, we studied the two methods applied to alanine dipeptide to compare convergence and barrier crossing in a simple real setting where the PMF can nonetheless be calculated accurately. Finally, we compared barrier crossing in the two in a practical setting, histidine gating in myoglobin. We also compared to metadynamics without tempering (untempered metadynamics, UTMetaD) to verify that TTMetaD is as fast to drive barrier crossing as UTMetaD and confirm that it avoids the trade-off between fast initial exploration and efficient convergence. We did not attempt to tune TTMetaD in these comparisons; our purpose in these initial tests is to show that untuned TTMetaD can perform as well or better than WTMetaD using rough heuristics. The question of how far TTMetaD can be pushed is a subject for future work.

3.1. Random 1D Surfaces. Approximating real system dynamics as overdamped Brownian motion along the CV coordinates makes an excellent heuristic for understanding metadynamics theoretically. Accordingly, Brownian dynamics in a few dimensions on an analytically defined potential surface makes a good first test case for new metadynamics methods before applying them to more realistic systems. We chose to begin our tests with one-dimensional systems for ease of prototyping; finding a barrier in 1D is a matter of taking a minimum over a predefined range. These tests investigated the speed, accuracy, and robustness of TTMetaD as compared to WTMetaD.

To test the robustness, it is necessary to test accuracy and speed on many different potential surfaces with a variety of characteristic barrier heights and barrier structures. For the tests reported here, we chose 48 potentials of the form

$$F(x) = c_0 + \sum_{n=1}^{10} c_n \sin(n\pi x) \tag{6}$$

for x confined to the interval $[0,2]$ and standardized so that the minimum over the accessible interval is zero using $c_0 = \min_{x\in[0,2]} \sum_{n=1}^{10} c_n \sin(n\pi x)$, with the c_n for $n \geq 1$ each chosen uniformly randomly and independently from $[0,5k_BT]$. The coefficients as well as positions for leftmost and rightmost basins and the barrier positions for each surface can be found in our Supporting Information (SI), and a representative set is illustrated in Figure 1. The dynamics of each system was Euler−Murayama integrated Brownian motion with a diffusion constant of 1 and a time step of 0.0001. Each surface was simulated for 32 time units in 16 independent runs each initialized from the bottom of the leftmost and deepest basin in the potential in each case shown here. The shallower rightmost basin was taken as the second primary basin. We also performed rightmost-initialized, leftmost-secondary simulations with similar results that we have chosen not to present because they add little further insight and confirm the same essential points.

Each system's metadynamics used McGovern−de Pablo boundary-corrected Gaussian hills[25] with a height of 0.05 and a width of 0.025 deposited every 20 timesteps. The relative performance of WTMetaD and TTMetaD was not substantially affected by these choices. The TTMetaD runs used $\Delta T = 2k_BT$, while three sets of WTMetaD runs used $\Delta T = 8k_BT$, $\Delta T = 16k_BT$, and $\Delta T = 32k_BT$, respectively. The choice for TTMetaD made little difference between k_BT and $6k_BT$; the choices for WTMetaD reflect a good choice for optimal convergence rate for small-barrier systems, $8k_BT$, optimal convergence rate overall, $16k_BT$, and a choice more tilted toward driving barrier crossing quickly, $32k_BT$.

The results of these simulations confirm that TTMetaD is more robust, more accurate, and faster to drive barrier crossings than WTMetaD. Figure 2 shows that the time to first barrier crossing is lower in TTMetaD whether the WTMetaD ΔT

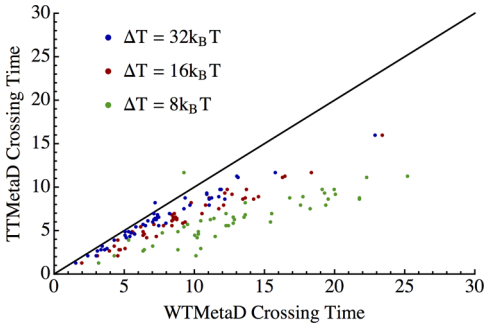

Figure 2. Comparison of first crossing times for TTMetaD with $\Delta T = 2k_BT$ and WTMetaD with a variety of ΔT parameters. With two exceptions in 144 comparisons, TTMetaD drives barrier crossing faster. On average, the speedup increases as the first crossing time increases.

parameter is chosen properly for average convergence, $16k_BT$, or chosen relatively high for fast barrier crossing, $32k_BT$. This confirms that it drives barrier crossing faster than WTMetaD systematically, robustly with respect to the multiwell barrier structure. Figure 3 shows that TTMetaD is systematically more precise than WTMetaD. In each figure, the spread of the TTMetaD results is narrower than the spreads for the WTMetaD results, confirming that the performance of TTMetaD is more robust to variance in the shape of the underlying potentials than WTMetaD. This is especially true for the low ΔT WTMetaD runs because, as is known in the literature, choosing ΔT to be higher than necessary makes for more robust convergence, but less accurate convergence when that robustness is not needed. TTMetaD all but eliminates that trade-off.

3.2. Alanine Dipeptide. Though overdamped dynamics makes a good heuristic guide, it is also necessary to test on more realistic systems. Alanine dipeptide is a common first test system for new enhanced sampling algorithms that exhibits many of the essential complexities common to more challenging biomolecular systems: high dimensionality, adequate but suboptimal choice of CVs, and imperfect separation of time scales between CVs and other variables. These tests cannot demonstrate robustness as directly as the previous tests did, as only one system is simulated. Instead, they are designed primarily to show that TTMetaD remains more precise and faster to drive barrier crossing than WTMetaD in more realistic systems. Alanine dipeptide is a standard first test for the accuracy of metadynamics methods[13] and will be our primary test of accuracy. The close relation of TTMetaD to WTMetaD and UTMetaD and previous experience with UTMetaD and WTMetaD then suggests that the relative accuracies of TTMetaD, WTMetaD, and UTMetaD on alanine dipeptide will be characteristic of those relative accuracies in more complex systems.

In these tests, we simulated biased blocked alanine dipeptide *in vacuo*, modeled by the CHARMM27 force field[32,33] and held at a constant temperature of 300 K using a Langevin thermostat with a drag of 5 amu/ps. The dynamics were simulated in Gromacs 4.6.1[28,34−36] using a stochastic dynamics leapfrog integrator with a time step of 2 fs, (superfluous) particle-mesh Ewald summation,[37] and SHAKE constraints on all bonds.[38] We performed 60 simulations for each metadynamics method presented. All simulations began from the same initial C_{7eq} conformation and the same pseudorandom Langevin force seed, but each set of 60 runs began from 60 distinct initial velocities pseudorandomly generated from different random seeds.

We compared UTMetaD, WTMetaD, TTMetaD, and ThTTMetaD using hill height, width, and rate parameters and WTMetaD tempering parameters tuned for WTMetaD in earlier work.[21] The height was 1.2 kJ/mol and the width 0.35 radians; hills were deposited every 120 fs, and the well-tempering parameter ΔT was 4 k_BT. For TTMetaD, we simply used a ΔT of 2 k_BT and for ThTTMetaD a ΔT of 2 k_BT and a threshold of 1 k_BT. The CVs were the ϕ and ψ angles, and the transition wells for TTMetaD were $(-1.25, 1.25)$ and $(1.0, -1.25)$ in CV coordinates: a rough, unoptimized choice of transition wells.

The results of these simulations confirm that TTMetad remains more precise and faster to drive barrier crossing than WTMetaD when applied to more realistic systems. Figure 4 shows the cumulative distribution function for first barrier crossing times for the various methods and parameters tested. These times closely follow log−logistic distributions for each tempered metadynamics method, as shown by the maximum likelihood best fits superimposed on each of the empirical distribution functions. The fits have two parameters each, a shape parameter that is the same to within error for all methods and a time scale parameter that is 30 ps for all the TTMetaD tests and 75 ps for optimized WTMetaD, indicating that TTMetaD is 2.5 times as fast to drive barrier crossings than WTMetaD in this test case. Surprisingly, we find that

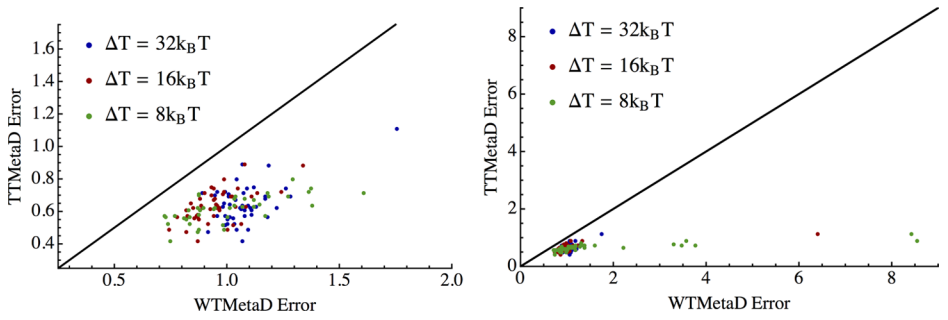

Figure 3. Comparison of accuracy for TTMetaD with $\Delta T = 2k_BT$ and WTMetaD with a variety of ΔT parameters. Error is measured as the maximum absolute value of the difference of the estimated PMF from the true potential in the between-basin region after both have been standardized to match in average potential value between the basins. The left panel shows a zoom on the main cluster of results and does not include all data points, while the right shows all results. With no exceptions in 144 cases, TTMetaD is more accurate than WTMetaD. Furthermore, while the spread of the WTMetaD accuracies decreases with higher ΔT, the spread of the TTMetaD accuracies is least of all.

dx.doi.org/10.1021/ct500441q | J. Chem. Theory Comput. 2014, 10, 3626−3633

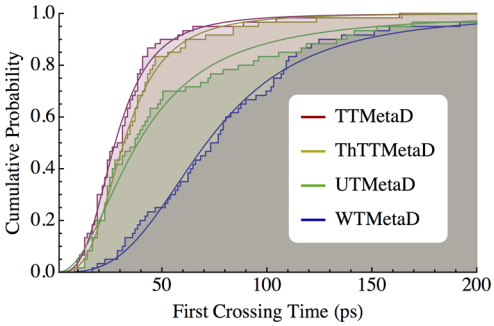

Figure 4. Cumulative distribution functions of first crossing times for blocked alanine dipeptide simulated using TTMetaD with $\Delta T = 2k_BT$, ThTTMetaD with $\Delta T = 2k_BT$ and $V_{th} = 1k_BT$, WTMetaD with $\Delta T = 4k_BT$, and metadynamics without tempering (UTMetaD), overlaid by maximum likelihood best fit log−logistic cumulative distribution function curves to guide the eye. The time to hitting the second basin is defined to the precision of the hill width, 0.35 radians, and the hill addition rate, 120 fs, for consistency with the underlying metadynamics algorithm.

TTMetaD is actually faster to drive barrier crossing than UTMetaD, not just as fast, especially in the tail of the distribution. Looking at the high variability of the bias in Figure 5, it seems possible that this may be due to excitation of orthogonal variables during relaxation after depositing large hills in high-energy regions. An orthogonal variable excitation could perturb the effective short-time mean forces and therefore perturb the effective barrier between wells, possibly preventing exploration of the target minimum. However, a full exploration of this surprising observation is beyond the scope of this work; our primary hypothesis, that TTMetaD is not slower to drive barrier crossing than UTMetaD, is confirmed by this test.

Figure 5 shows the means and standard deviations of the distributions of between-basin free energy estimates for each of the methods. The final standard deviation of the TTMetaD estimates is 0.41 ± 0.05 kJ/mol, while the standard deviation of the WTMetaD estimates is 0.6 ± 0.1 kJ/mol, indicating that TTMetaD offers an approximately 30% improvement in precision after 8 ns; the improvement at earlier times is comparable. The trueness of the TTMetaD estimates, especially the ThTTMetaD estimates, is also better than that for the WTMetaD estimates after 500 ps when the precision becomes roughly equal to k_BT, but precision rather than trueness is always the limiting factor on accuracy after this point. ThTTMetaD trueness is superior compared to TTMetaD because it shows less of a problem with undershooting the barrier after the first overshoot, which corresponds to the idea that the threshold allows it to drive recrossing more reliably. However, this does not appear to be a major effect in this system. Finally, examining the curves in Figure 5 shows that the WTMetaD data show coarser, more visible noise, indicating higher autocorrelation in the basin−basin free energy difference estimates. Such autocorrelation can confound free energy estimation, so a less-correlated estimator is preferable. The difference in autocorrelation may arise from the fact that TTMetaD fully flattens the free energy surface, whereas WTMetaD only partially flattens it. The relative autocorrelations of the estimators should reflect the relative autocorrelations of the biased peptide dynamics.

3.3. Myoglobin. Finally, we compared the methods in tests on a small protein, myoglobin, because blocked alanine dipeptide does not exhibit the full dynamical richness of larger biomolecules and methods validated on alanine dipeptide do not always transfer well to more complex systems. Our target for the test was a rotameric transition in histidine 64 that has been discussed as gating the diffusion of gas molecules into and out of the heme binding pocket. As with the blocked alanine dipeptide simulations, these tests do not demonstrate robustness directly, as only one system is simulated. These tests are specifically designed to show that TTMetaD is faster to drive barrier crossing than WTMetaD, even more in complex systems than in the dipeptide, and to check the cost of pathfinding in a complex calculation. They use unoptimized CVs for which we are not interested in a PMF, so we do not run the tests to convergence.

In these tests, we simulated oxygenated, heme-bound biased myoglobin in water, with protein governed by the CHARMM27 force field[32,33] and water by the TIP3P model,[39] held at a constant temperature of 300 K using a stochastic velocity rescaling thermostat[40] with a time constant of 5 ps. The dynamics were simulated in Gromacs 4.6.1[28,34−36] using a leapfrog integrator with a time step of 2 fs, particle-mesh Ewald summation,[37] and LINCS constraints on all bonds.[41,42] We performed 24 simulations for each metadynamics method and parameter set presented. All simulations began from the same initial conformation and the same pseudorandom stochastic velocity rescaling force seed, but each set of 24 runs began from 24 distinct initial velocities pseudorandomly generated from different random seeds. The initial conformations were generated from the PDB structure

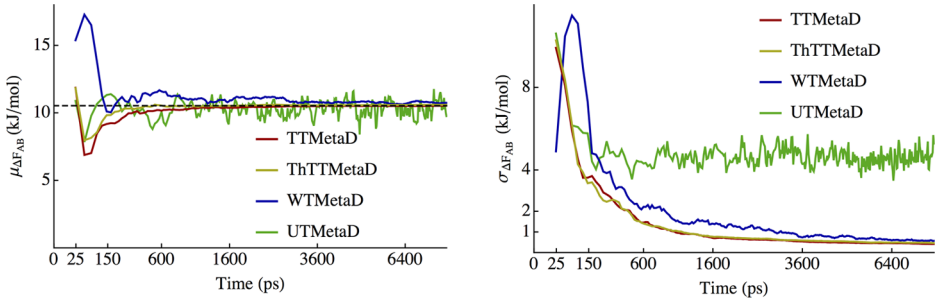

Figure 5. Time series of the means and standard deviations of the between-basin free energy difference estimates for the simulations of blocked alanine dipeptide using TTMetaD with $\Delta T = 2k_BT$, ThTTMetaD with $\Delta T = 2k_BT$ and $V_{th} = 1k_BT$, WTMetaD with $\Delta T = 4k_BT$, and metadynamics without tempering (UTMetaD); dashed line in left panel shows target result. Times are plotted on a square root scale to emphasize initial transients. Though TTMetaD and ThTTMetaD are roughly equally precise at all times, ThTTMetaD is more true earlier. WTMetaD is systematically less true and less precise and has higher confounding autocorrelation; UTMetaD does not converge.

dx.doi.org/10.1021/ct500441q | J. Chem. Theory Comput. 2014, 10, 3626−3633

1MBO,[43] using Gromacs built-in tools to add hydrogens and 9055 solvent waters and to minimize the energy of the system after adding hydrogens and solvent.

In this test, we compared only WTMetaD and TTMetaD. The CVs were the χ_1 and χ_2 angles of histidine 64. We chose to simulate this using similar parameters as for alanine dipeptide, as the CVs are similar and the transition wells for TTMetaD were the same as before, $(-1.25, 1.25)$ and $(1.0, -1.25)$ in CV coordinates. A single WTMetaD run of 20 ns validated the choice of transition wells before running the TTMetaD. However, because the protein is a more sensitive dynamical environment we made the initial rate of bias addition an order of magnitude slower. The hill heights were 0.3 kJ/mol, the widths 0.35 radians; hills were deposited every 300 fs, and the well-tempering ΔT was 4 $k_B T$. For TTMetaD, we once again used a ΔT of 2 $k_B T$.

Once again, we found that TTMetaD is systematically faster to drive transitions than WTMetaD and is in fact no slower than UTMetaD, the best-case result, as shown in Figure 6. In addition, in these tests we can compare running times meaningfully; here the performance measured in nanoseconds per day unexpectedly increased by approximately 1% from WTMetaD and UTMetaD to TTMetaD, but more expectedly the difference does not appear significant. By design, these tests cannot demonstratively confirm that any of the methods is more accurate or more precise than the others, but we note that there is no set of parameters for which the UTMetaD simulation would converge, so the fact that TTMetaD is no slower for exploration than UTMetaD is strong support for its overall superiority for free energy estimation.

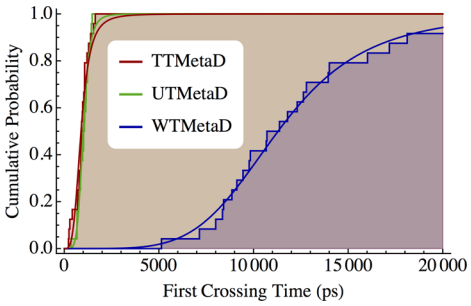

Figure 6. Cumulative distribution functions of first crossing times for simulations of myoglobin using TTMetaD with $\Delta T = 2k_B T$, WTMetaD with $\Delta T = 4k_B T$, and untempered metadynamics, overlaid by maximum likelihood best fit log−logistic cumulative distribution function curves to guide the eye. The time to hitting the second basin is defined to the precision of the hill width, 0.35 radians, and the hill addition rate, 300 fs, for consistency with the underlying metadynamics algorithm.

Figure 6 shows that in this case TTMetaD is an order of magnitude faster to drive a barrier crossing than WTMetaD. This likely indicates that the WTMetaD ΔT is too small. However, the fact that the TTMetaD ΔT proves more transferable is one of the advantages of the method, so the comparison is representative of practice. UTMetaD is a limit of TTMetaD and WTMetaD, so this indicates that TTMetaD's exploration rate is insensitive to ΔT over the range $[2kT, \infty]$ while WTMetaD's varies by an order of magnitude over the range $[4kT, \infty]$. WTMetaD is thus more difficult to tune correctly. Notably, the WTMetaD times remain log−logistically distributed, while TTMetaD and UTMetaD appear to give rise to much narrower long-time tails, suggesting that TTMetaD may offer disproportionate improvements in the reproducibility of barrier crossing times compared to its improvements in speed when barriers are higher. This advantage is especially important for preliminary exploratory research in which one would like to limit the amount that simple randomness can confound one's investigation of the proper choice of CVs and parameters.

4. CONCLUSIONS

In this article, we have introduced a new form of metadynamics that uses an on-the-fly estimate of the free energy between basins (V^*) to tune the size of the hills in a way that ensures the basins are escaped as fast as possible relative to the original metadynamics without compromising on convergence rate relative to WTMetaD. In our tests, the method consistently improves upon WTMetaD in both speed and accuracy. Moreover, it is more robust and can be parametrized using more commonly available prior knowledge. Instead of requiring an estimate for the energy barrier, to first approximation it requires only the CV-space coordinates of one point in each of the basins separated by the barrier. These advantages would make TTMetaD a superior choice for studying transitions with known end states but an unknown mechanism, and especially superior in the case that the choice of CVs is not certain. In such a case, it is essential to get a quick estimate of the biased barrier crossing mechanism to check the quality of the CVs. TTMetaD reveals the barrier-crossing mechanism for a given choice of CVs more quickly than WTMetaD would, and potentially more reproducibly if our findings for myoglobin generalize to other highly complex systems. These efficiency gains will provide the highest impact in situations where simulation is most expensive, for instance in *ab initio* molecular dynamics and QM/MM sampling.

The novel transition-based on-the-fly tuning strategy used in TTMetaD may also be translatable into strategies for improving other adaptive biasing methods such as Adaptive Biasing Force,[14] Wang−Landau,[16] or Orthogonal Space Random Walk.[44] It is closely related in concept to the Wang−Landau flat histogram criterion strategy, which has previously been used with metadynamics,[45] but it operates in a more continuous manner and automatically flattens only an adaptively determined minimal metabasin region rather than a preselected CV region containing that minimal metabasin. Therefore, it can offer computational savings and requires less foreknowledge of the system to apply. One interesting possibility would be to use V^* to trigger the second phase of flux-tempered metadynamics[46] after using TTMetaD during the first phase. A method based on that hybrid approach may converge yet more rapidly relative to WTMetaD than the current method. A second would be to use V^* to tune the nonequilibrium driving forces in driven metadynamics,[47] a method that may drive first barrier crossing events even more rapidly and increase convergence rate even further by decreasing state-to-state round trip time scales.

In developing TTMetaD, we were careful to make sure that it retained the full flexibility of WTMetaD. TTMetaD can be used with adaptively sized hills,[21] field-coordinate CVs,[26] boundary-corrected hills,[25] driving forces,[47] and bias-exchange,[48] among others; few advances for WTMetaD cannot also be used with TTMetaD. In fact, we implemented it in PLUMED[27] to make it easy to use and familiar for current practitioners of metadynamics, and we implemented it in a modular way so that it can already be used with all of the enhancements

described above that are included in PLUMED. Our implementation code is freely available on request and is open for use and modification.

However, whatever the cost of an enhanced sampling method in raw computational resources, and whatever the potential efficiency gains, it is nearly always the case that the effort required to understand and apply it—the time and training of students—is in fact the limiting resource that must be economized most carefully in research efforts in this field. With that in mind, TTMetaD has been designed to be as easy to use as metadynamics, easier to use than WTMetaD, and compatible with existing metadynamics workflows to the maximum extent possible. With existing technology any lab already using metadynamics and PLUMED can begin using TTMetaD simply by reinstalling PLUMED with any compatible MD engine, changing one line of an existing PLUMED input file, and running the corresponding simulation otherwise as normal.

■ ASSOCIATED CONTENT

Supporting Information

The table of particular random coefficients used to define the 1D potential surface tests is provided. This material is available free of charge via the Internet at http://pubs.acs.org.

■ AUTHOR INFORMATION

Corresponding Author

*E-mail: jfdama@uchicago.edu.

Present Address

[‖]Biophysics Graduate Group, University of California, Berkeley, California 94720, United States

Notes

The authors declare no competing financial interest.

■ ACKNOWLEDGMENTS

This material is based upon work supported by the National Science Foundation (NSF grant CHE-1214087) and the European Union (grant ERC-2009-AdG-247075).

■ REFERENCES

(1) Karplus, M.; McCammon, J. A. *Nat. Struct. Biol.* **2002**, *9*, 646−52.
(2) Adcock, S. A.; McCammon, J. A. *Chem. Rev.* **2006**, *106*, 1589−615.
(3) Shaw, D. E.; Maragakis, P.; Lindorff-Larsen, K.; Piana, S.; Dror, R. O.; Eastwood, M. P.; Bank, J. A.; Jumper, J. M.; Salmon, J. K.; Shan, Y.; Wriggers, W. *Science* **2010**, *330*, 341−6.
(4) Kollman, P. *Chem. Rev.* **1993**, *93*, 2395−2417.
(5) Christ, C. D.; Mark, A. E.; van Gunsteren, W. F. *J. Comput. Chem.* **2009**, *31*, 1569−1582.
(6) Abrams, C.; Bussi, G. *Entropy* **2013**, *16*, 163−199.
(7) Torrie, G.; Valleau, J. *J. Comput. Phys.* **1977**, *23*, 187−199.
(8) Kästner, J. *Wiley Interdiscip. Rev.: Comput. Mol. Sci.* **2011**, *1*, 932−942.
(9) Mezei, M. *J. Comput. Phys.* **1987**, *68*, 237−248.
(10) Bartels, C.; Karplus, M. *J. Comput. Chem.* **1997**, *18*, 1450−1462.
(11) Laio, A.; Parrinello, M. *Proc. Natl. Acad. Sci. U. S. A.* **2002**, *99*, 12562−6.
(12) Laio, A.; Gervasio, F. L. *Rep. Prog. Phys.* **2008**, *71*, 126601.
(13) Barducci, A.; Bonomi, M.; Parrinello, M. *Wiley Interdiscip. Rev.: Comput. Mol. Sci.* **2011**, *1*, 826−843.
(14) Darve, E.; Pohorille, A. *J. Chem. Phys.* **2001**, *115*, 9169.
(15) Darve, E.; Rodrguez-Gómez, D.; Pohorille, A. *J. Chem. Phys.* **2008**, *128*, 144120.
(16) Wang, F.; Landau, D. *Phys. Rev. Lett.* **2001**, *86*, 2050−2053.
(17) Huber, T.; Torda, A. E.; van Gunsteren, W. F. *J. Comput.-Aided Mol. Des.* **1994**, *8*, 695−708.
(18) Barducci, A.; Bussi, G.; Parrinello, M. *Phys. Rev. Lett.* **2008**, *100*, 020603.
(19) Belardinelli, R.; Pereyra, V. *Phys. Rev. E* **2007**, *75*, 046701.
(20) Robbins, H.; Monro, S. *Ann. Math. Stat.* **1951**, *22*, 400−407.
(21) Branduardi, D.; Bussi, G.; Parrinello, M. *J. Chem. Theory Comput.* **2012**, *8*, 2247−2254.
(22) Dama, J. F.; Parrinello, M.; Voth, G. A. *Phys. Rev. Lett.* **2014**, *112*, 240602.
(23) Laio, A.; Rodriguez-Fortea, A.; Gervasio, F. L.; Ceccarelli, M.; Parrinello, M. *J. Phys. Chem. B* **2005**, *109*, 6714−21.
(24) Bussi, G.; Laio, A.; Parrinello, M. *Phys. Rev. Lett.* **2006**, *96*, 090601.
(25) McGovern, M.; de Pablo, J. *J. Chem. Phys.* **2013**, *139*, 084102.
(26) Tribello, G. A.; Ceriotti, M.; Parrinello, M. *Proc. Natl. Acad. Sci. U. S. A.* **2012**, *109*, 5196−201.
(27) Bonomi, M.; Branduardi, D.; Bussi, G.; Camilloni, C.; Provasi, D.; Raiteri, P.; Donadio, D.; Marinelli, F.; Pietrucci, F.; Broglia, R. A.; Parrinello, M. *Comput. Phys. Commun.* **2009**, *180*, 1961−1972.
(28) Berendsen, H.; van der Spoel, D.; van Drunen, R. *Comput. Phys. Commun.* **1995**, *91*, 43−56.
(29) Plimpton, S. *J. Comput. Phys.* **1995**, *117*, 1−19.
(30) Phillips, J. C.; Braun, R.; Wang, W.; Gumbart, J.; Tajkhorshid, E.; Villa, E.; Chipot, C.; Skeel, R. D.; Kalé, L.; Schulten, K. *J. Comput. Chem.* **2005**, *26*, 1781−802.
(31) Dijkstra, E. W. *Numer. Math* **1959**, *1*, 269−271.
(32) MacKerell, A. D.; Bashford, D.; Bellott, M.; Dunbrack, R. L.; Evanseck, J. D.; Field, M. J.; Fischer, S.; Gao, J.; Guo, H.; Ha, S.; Joseph-McCarthy, D.; Kuchnir, L.; Kuczera, K.; Lau, F. T. K.; Mattos, C.; Michnick, S.; Ngo, T.; Nguyen, D. T.; Prodhom, B.; Reiher, W. E.; Roux, B.; Schlenkrich, M.; Smith, J. C.; Stote, R.; Straub, J.; Watanabe, M.; Wiórkiewicz-Kuczera, J.; Yin, D.; Karplus, M. *J. Phys. Chem. B* **1998**, *5647*, 3586−3616.
(33) MacKerell, A. D.; Feig, M.; Brooks, C. L. *J. Comput. Chem.* **2004**, *25*, 1400−15.
(34) Lindahl, E.; Hess, B.; van der Spoel, D. *J. Mol. Model.* **2001**, *7*, 306−317.
(35) Van Der Spoel, D.; Lindahl, E.; Hess, B.; Groenhof, G.; Mark, A. E.; Berendsen, H. J. C. *J. Comput. Chem.* **2005**, *26*, 1701−18.
(36) Hess, B.; Kutzner, C.; van der Spoel, D.; Lindahl, E. *J. Chem. Theory Comput.* **2008**, *4*, 435−447.
(37) Essmann, U.; Perera, L.; Berkowitz, M. L.; Darden, T.; Lee, H.; Pedersen, L. G. *J. Chem. Phys.* **1995**, *103*, 8577.
(38) Ryckaert, J.-P.; Ciccotti, G.; Berendsen, H. J. *J. Comput. Phys.* **1977**, *23*, 327−341.
(39) Jorgensen, W. L.; Chandrasekhar, J.; Madura, J. D.; Impey, R. W.; Klein, M. L. *J. Chem. Phys.* **1983**, *79*, 926.
(40) Bussi, G.; Donadio, D.; Parrinello, M. *J. Chem. Phys.* **2007**, *126*, 014101.
(41) Miyamoto, S.; Kollman, P. a. *J. Comput. Chem.* **1992**, *13*, 952−962.
(42) Hess, B. *J. Chem. Theory Comput.* **2008**, *4*, 116−122.
(43) Phillips, S. E. *J. Mol. Biol.* **1980**, *142*, 531−554.
(44) Zheng, L.; Chen, M.; Yang, W. *Proc. Natl. Acad. Sci. U. S. A.* **2008**, *105*, 20227−32.
(45) Min, D.; Liu, Y.; Carbone, I.; Yang, W. *J. Chem. Phys.* **2007**, *126*, 194104.
(46) Singh, S.; Chiu, C.-c.; de Pablo, J. J. *J. Stat. Phys.* **2011**, *145*, 932−945.
(47) Moradi, M.; Tajkhorshid, E. *J. Phys. Chem. Lett.* **2013**, *4*, 1882−1887.
(48) Piana, S.; Laio, A. *J. Phys. Chem. B* **2007**, *111*, 4553−9.